Available online at www.sciencedirect.com
SCIENCE DIRECT®
Journal of Power Sources 139 (2005) 182–187
JOURNAL OF POWER SOURCES
www.elsevier.com/locate/jpowsour

Short communication

Oxidation of Haynes 230 alloy in reduced temperature solid oxide fuel cell environments

Li Jian[a,b,*], Pu Jian[a,b], Xiao Jianzhong[a,b], Qian Xiaoliang[b]

[a] *College of Materials Science and Engineering, Huazhong University of Science and Technology, 1037 Luo Yu Lu Wuhan, Hubei 430074, China*
[b] *Fuel Cell Research Institute, Huazhong University of Science and Technology, 1037 Luo Yu Lu Wuhan, Hubei 430074, China*

Received 22 June 2004; accepted 19 July 2004
Available online 22 September 2004

Abstract

Haynes 230 alloy was exposed to reducing and oxidizing environments at 750 °C for 1000 h, simulating the conditions in a reduced temperature solid oxide fuel cell (SOFC). The oxidized specimens were characterized in terms of the oxide morphology, composition and crystal structure. The oxide scale in each environment was identified as Cr_2O_3 with the existence of Cr_2MnO_4. Ni remained metallic in the reducing atmosphere, and NiO was detected in the sample exposed to air. The oxide scale is around 1 μm thick after 1000 h of oxidation in both situations. The area specific resistance (ASR) contributed by the oxide scale is expected less than 0.1 Ω cm^2 after 40,000 h of exposure when a parabolic oxide growth rate is assumed, demonstrating the suitability of the interconnect application of this alloy in the reduced temperature SOFCs.

Keywords: Ni-based alloy; Interconnects; Solid oxide fuel cells; Area specific resistance; Oxidation

1. Introduction

Solid oxide fuel cells (SOFCs) offer a high-energy conversion efficiency of fossil fuels to electricity at a low emissions level. With a high operating temperature in the range of 600–1000 °C, the fossil fuels can be directly internally reformed to provide hydrogen to the fuel cell, eliminating the need for an external reformer and allowing increased compactness. Furthermore, rapid kinetics can be achieved with non-precious electrode materials and high quality heat is produced as a byproduct for co-generation.

However, the high temperature of the SOFC places rigorous requirements on its component materials. Among the most critical needs for the commercial deployment of SOFCs are the interconnects, which separate the fuel and oxidant and provide electric connection between the anode and cathode of adjacent cells. Close thermal expansion match to the fuel cell components, sufficient electronic conduction at the operation temperature, good chemical stability in both reducing and oxidizing environments and adequate thermal cyclicability are fundamental requirements. Previously, interconnect materials for SOFCs operated at ∼1000 °C are complex perovskite ceramic oxides, typically, the Sr- or Ca-doped $LaCrO_3$ [1]. However, this ceramic interconnect is mechanically brittle, difficult to manufacture in a large planar form, deforms due to the loss of oxygen at the fuel-side, and represents a significant portion of the product cost in a planar SOFC stack design. Therefore, metallic-type interconnects for planar SOFCs are desirable, offering excellent ductility, higher electronic conductivity, higher heat conductivity, lower cost and flexible fabricability. In turn, significant performance and cost advantage can be realized.

So far, metallic interconnects have not been successfully deployed, since the oxidation of metallic materials forms an electrically insulating surface oxide, leading to undesirable increase in contact electrical resistance. Furthermore, the incompatibility in thermal expansion between the metal-

* Corresponding author. Tel.: +86 27 8754 4307; fax: +86 27 8754 4650.
E-mail address: plumarror@yahoo.com (L. Jian).

0378-7753/$ – see front matter © 2004 Elsevier B.V. All rights reserved.
doi:10.1016/j.jpowsour.2004.07.019

lic interconnect and cell component materials (electrolyte and electrodes) causes the interfacial contact breakdown. A Cr-based alloy, Cr–5Fe–1Y_2O_3, manufactured by Plansee Ltd., is a well-known metallic material proposed for planar high-temperature SOFC interconnect. It is a pre-alloyed ODS powder; therefore, material cost is significant. The sintered Cr–5Fe–1Y_2O_3 offers thermal expansion compatibility with stabilized zirconia and excellent oxidation resistance [2], however, rapid electrochemical degradation was observed with this Plansee interconnect. This degradation was found to be related to the evaporation of Cr from the interconnect followed by its deposition on the cathode surface [3].

Recent progress in reduced temperature SOFCs (<800 °C) have provided a valuable opportunity for replacing the ceramic interconnects by metallic alloys. The reduced temperature SOFCs that maintain the cell power density and durability at the same level as those operated at temperatures near 1000 °C are achieved by reducing the thickness of the electrolyte [4,5], and/or by the identification of new electrolytes with improved oxygen ion conductivity [5–8]. High-temperature oxidation-resistant alloys are generally considered to be the candidate materials for reduced temperature SOFC interconnects [9–13]. Such alloys contain Cr and/or Al as the alloying elements to form a protective oxide scale, by preferential oxidation of Cr (Cr_2O_3) or Al (Al_2O_3). Al_2O_3-forming alloys are less interesting for SOFC interconnect application due to the low electrical conductivity of the oxide scale. Studies have focused on the Cr_2O_3-forming alloys, especially the Cr-containing ferritic stainless steels [14–29] with a thermal expansion coefficient in the neighborhood of 12×10^{-6}. Austenitic alloys, such as austenitic stainless steels and superalloys [30,31] have rarely evaluated as an interconnect candidate material due to their relatively high thermal expansion coefficients.

In the present paper, Haynes 230, a Ni-based alloy, was investigated in the SOFC environments. Special attention was given to the oxidation behavior in both oxidizing (cathode) and reducing (anode) atmospheres, including the morphology, thickness, crystal structure, and composition of the oxide scales. The purpose of the present study is to examine the possibility of Haynes 230 for the interconnect application in the reduced temperature SOFCs. Haynes 230 has a mean coefficient of thermal expansion (CTE) 15.2×10^{-6} between 25 and 800 °C [32], which is slightly higher than that of the SOFC cell components ((10–13) $\times 10^{-6}$ [33]), however, the difficulty caused by the minor mismatch in CTEs can be alleviated through the design of the SOFC stack configuration.

2. Experimental procedures

A Ni-based alloy, Haynes 230, with an nominal composition (in wt.%) 57Ni–22Cr–14W–2Mo–0.5Mn–0.4Si–0.3Al–0.10C–0.02La–5Co–3Fe–0.015B, was provided by Liyuan Precision Materials Ltd. Coupon specimens with dimensions of 20 mm × 20 mm × 1 mm were cut by using a Buhler slow diamond saw, and were placed in an atmosphere controlled furnace for oxidation in both oxidizing and reducing environments, respectively, simulating the cathode (air) and anode (humidified H_2) conditions in a reduced temperature SOFC. The oxidation temperature was 750 °C, and the oxidation duration was 1000 h.

Small specimens with dimensions of 5 mm × 5 mm × 1 mm were obtained from the oxidized samples for the observation of the surface morphology of the oxide scales; the samples for the cross-section examination were mounted in a Buhler epoxide and polished on a Buhler automatic polisher. A D/Max-3B X-ray diffractometer was employed to identify the crystal structure of the oxide; a JSM-5510LV scanning electron microscope (SEM) with energy dissipation spectrum (EDS) attachment was used for the oxide scale examination.

3. Results and discussions

3.1. Oxidation in oxidizing (cathode) environment

Fig. 1 shows the typical morphology of the surface oxide scale of Haynes 230 exposed to air at 750 °C for 1000 h, which consists of fine oxide particles and is much more compact than that formed in the SS 430 and other ferritic stainless steels in similar conditions. The EDS result obtained from the surface, shown in Fig. 2, indicates that the oxide scale may contain O, Cr, Mn, Ni and insignificant amount of W and other elements. The electrons penetrated the oxide scale, X-rays might also be generated from the substrate, and therefore, the exact oxide composition cannot be determined in this way. However, compared with the substrate composition, it can be seen that the Cr and Mn contents in the oxide scale are significantly higher than that in the substrate, indicating Cr and Mn outward migrations to the surface and subsequent oxidation. Fig. 3 is a typical cross-section SEM micrograph of the oxidized Haynes 230 exposed to air at 750 °C for 1000 h. It confirms a very thin oxide scale of ~1 μm. At the oxide scale/substrate interface, no voids and cracks are observed,

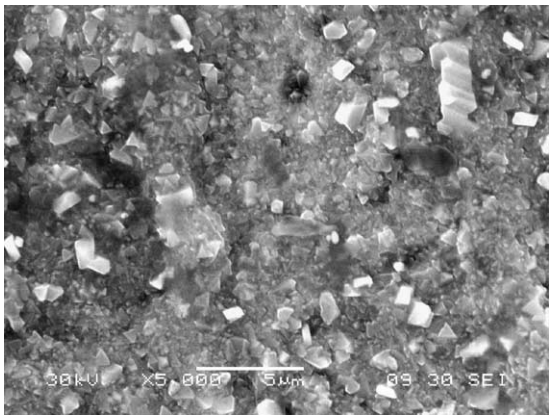

Fig. 1. SEM micrograph of the surface oxide of Haynes 230 exposed to air at 750 °C for 1000 h, showing a dense oxide scale with fine particles.

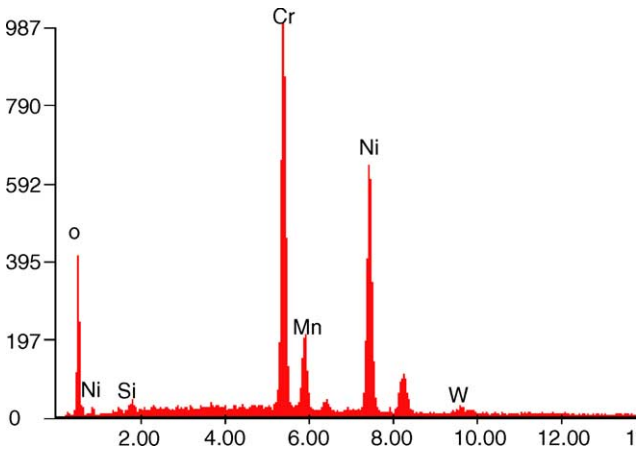

Fig. 2. EDS spectrum taken from the oxidized surface shown in Fig. 1.

suggesting a continuous formation of oxide scale from the substrate and a good adhesion to the alloy. The gap above the oxide scale was formed due to the shrinkage of the epoxide used to mount the sample.

Fig. 4 is the X-ray diffraction pattern obtained from the oxidized surface. Other than the substrate, the oxide scale is predominantly Cr_2O_3; spinel type Cr_2MnO_4 and NiO are also identified, using the corresponding standard diffraction data published by JCPDS-ICDD. Due to the thin nature of the oxide scale, the oxide diffraction peaks are relatively small compared with that of the substrate.

3.2. Oxidation in reducing (anode) environment

Fig. 5 shows the surface oxide morphology of Haynes 230 exposed to the reducing anode environment (moisturized H_2) at 750 °C for 1000 h. An oxidation phenomenon was found that is very different from that observed in air, shining nodules were developed besides the oxides; the nodules were preferably formed within the grains, depicting a grain boundary network. Under a higher magnification, Fig. 6, a dense oxide scale with fine oxide particles is shown. Both

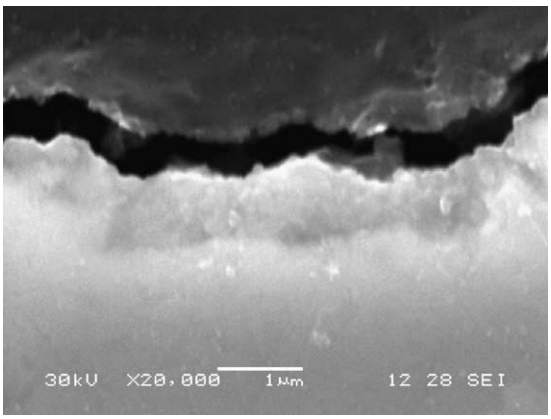

Fig. 3. SEM micrograph of the cross-section of Haynes 230 exposed to air at 750 °C for 1000 h, showing an oxide scale thickness around 1 μm.

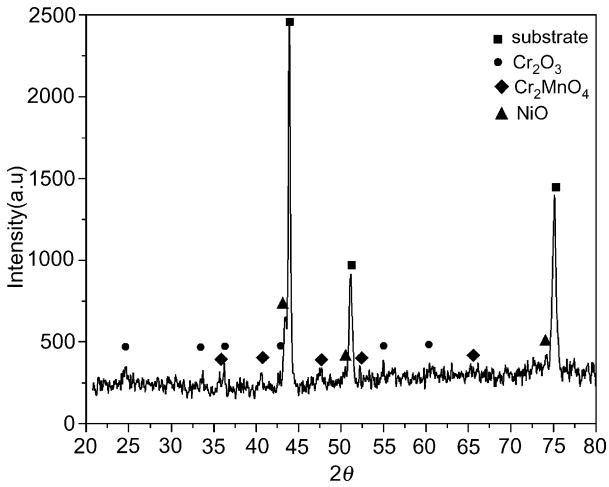

Fig. 4. X-ray diffraction pattern taken from the oxidized surface shown in Fig. 1.

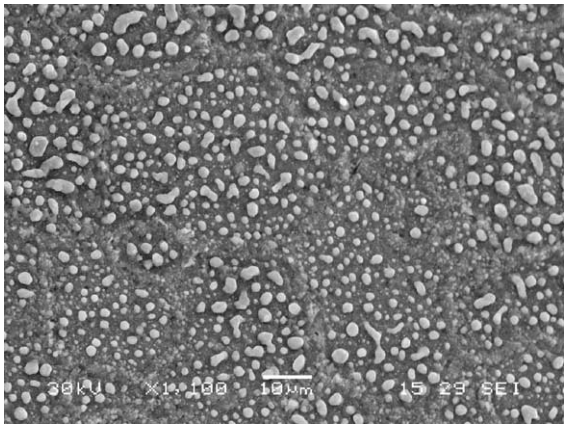

Fig. 5. SEM micrograph of the surface morphology of Haynes 230 exposed to the reducing atmosphere at 750 °C for 1000 h.

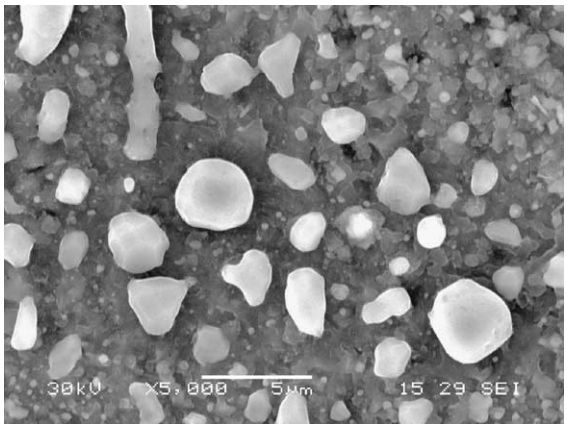

Fig. 6. Higher magnification SEM micrograph of the surface oxide of Haynes 230 exposed in the reducing atmosphere at 750 °C for 1000 h, showing a dense oxide scale with fine particles.

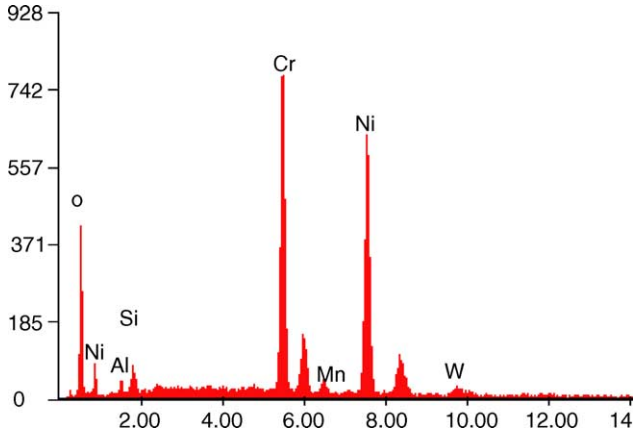

Fig. 7. EDS spectrum taken from the oxidized surface shown in Fig. 7.

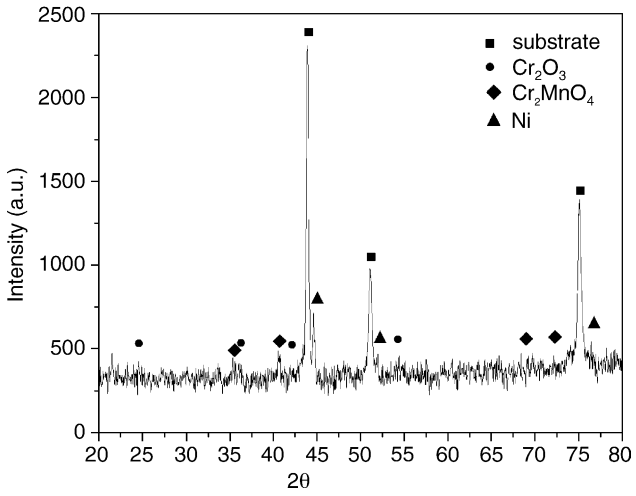

Fig. 9. X-ray diffraction pattern taken from the oxidized surface shown in Fig. 6.

the grain boundary and grain oxides have similar compositions revealed by the EDS analysis, containing Cr, Mn, and O, as shown in Fig. 7 where the Ni signals were generated either from the substrate or the surrounding nodules, which will be explained latter. Fig. 8 is a cross-section micrograph of the alloy oxidized in the reducing anode environment; it confirms a thin, dense and adhesive oxide layer with a thickness close to 1 μm, in the same order of that formed in the cathode environment. Therefore, it can be concluded that the oxidation in the anode side is not less significant than that in the cathode side within a reduced temperature SOFC.

Fig. 9 is the X-ray diffraction pattern taken from the oxidized surface, indicating the existence of Cr_2O_3, Cr_2MnO_4 and pure Ni other than the substrate. The Ni existence in the oxide scale was not reported in previous study [31] where Haynes 230 was oxidized in the temperature range of 700–1100 °C for up to 1000 h in humidified H_2. As known, in order to oxidize Ni to NiO, the oxygen activity must exceed a certain equilibrium value that varies with temperature. At 750 °C, the oxygen partial pressure for forming NiO is $\sim 10^{-16}$ atm [34], which is expected to be much higher than that in the moistured H_2 used in the test. According to Ref. [31], for wet hydrogen bubbled through water at 40 °C, the oxygen partial pressure at 750 °C is in the range between 3.3×10^{-21} and 1.1×10^{-23}. Therefore, the Ni remained metallic after 1000 h exposure to the environment, while Cr was selectively oxidized. Fig. 10 shows the cross-section of a nodule on top of the oxide scale, and the EDS analysis at the nodule, as seen in Fig. 11, confirms that the nodule is composed of pure Ni; and the Cr signal is from the surrounding oxide or substrate since the signal was generated in a pear-like volume that is bigger than the nodule size. When the Cr oxide is nucleated on the original alloy surface, it grows inward by the outward diffusion of Cr; the Ni is rejected and enriched at the alloy/scale interface. Due to the volume expansion associated with the Cr to Cr_2O_3 reaction, the ejected Ni is under compression, subsequently diffuses towards the free surface where it has a lower free energy, and forms nodules. It is expected that a complete layer of Ni will be formed with further oxidation as demonstrated in the case of the superalloy oxidation in the molten carbonate fuel cells [35]. At the grain boundaries, the vacancy concentration is expected to be higher than that in the grains, and the rejected Ni may

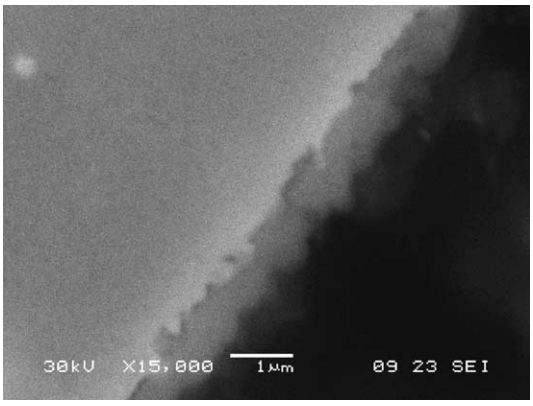

Fig. 8. SEM micrograph of the cross-section of Haynes 230 exposed in the reducing atmosphere at 750 °C for 1000 h, showing an oxide scale thickness around 1 μm.

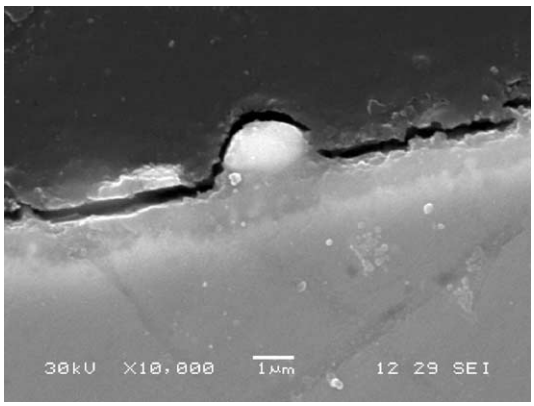

Fig. 10. SEM micrograph showing the cross-sectioned Ni nodule on top of the oxide scale on the surface oxidized in the reducing atmosphere.

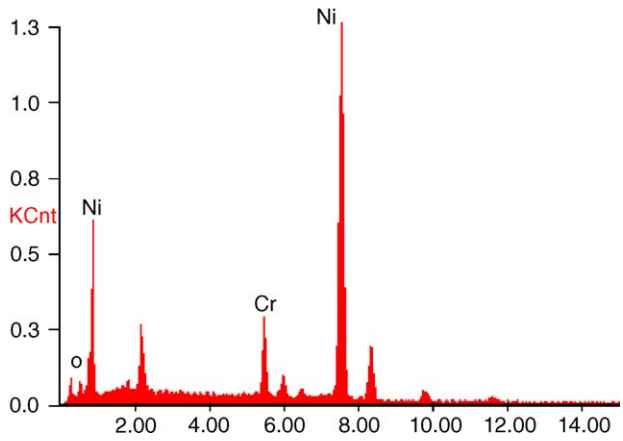

Fig. 11. EDS spectrum taken from the Ni nodule shown in Fig. 10.

stay inside the grain boundaries, instead of forming nodules on top of the surface.

3.3. Area specific resistance

With the oxidation of the metallic interconnect materials, the oxide scale gradually builds up on the surface of the interconnect, and increases the ASR with time. The ASR contributed by the interconnect oxidation can be expressed by

$$\mathrm{ASR} = \rho t \quad (1)$$

where ρ is the electrical resistivity of the oxide, and t the oxide thickness. Commonly, it is considered that an ASR below 0.1 $\Omega\,cm^2$ contributed by the metallic interconnect is acceptable [10]. Since the oxides formed in both reducing and oxidizing environments are predominantly Cr_2O_3, it is reasonable to evaluate the ASR according to the resistivity of Cr_2O_3. Taking the value of $\rho(Cr_2O_3)$ as ~78 Ω cm at 750 °C [36], the ASR after 1000 h exposure to the SOFC environments will be $15.6 \times 10^{-3}\ \Omega\,cm^2$ when the oxide scale thickness is around 1 μm on each side and the electrical resistance of the substrate alloy is negligible. If it is assumed that the growth rate of the oxide scale follows the parabolic law, as confirmed in previous studies [30,31], the thickness of the oxide scale on each side will be 6.32 μm after 40,000 h exposure, and the ASR then will be 0.098 $\Omega\,cm^2$, which is less than the conventionally acceptable value of the ASR. Therefore, it can be concluded that Haynes 230 alloy is suitable for the interconnect application in a SOFC operated at 750 °C for 40,000 h.

4. Conclusions

From the oxidation study of Haynes 230 alloy in the reducing and oxidizing environments similar to the conditions in the reduced temperature SOFCs, the following conclusions are made:

(1) Haynes 230 alloy has an excellent oxidation resistance in both anode and cathode environments of a SOFC operated at 750 °C. Exposed to the environments for 1000 h, a dense oxide scale around 1 μm formed.
(2) In the reducing anode atmosphere, the oxide is predominantly Cr_2O_3 with some spinel Cr_2MnO_4; in the oxidizing cathode atmosphere, the oxide is basically Cr_2O_3 with some Cr_2MnO_4 and NiO.
(3) The oxygen partial pressure in the anode environment is less than that needed to oxidize Ni at 750 °C, Ni remained metallic and formed nodules on top of the oxidized surface.
(4) The ASR contributed by the oxide scales on Haynes 230 is expected to be less than 0.1 $\Omega\,cm^2$ after being exposed to the SOFC environments at 750 °C for 40,000 h, and therefore, Haynes 230 is suitable for the interconnect application in the reduced temperature SOFCs.

Acknowledgement

This research was financially supported by the National Science Foundation of China.

References

[1] N.Q. Minh, T. Takahashi, Science and Technology of Ceramic Fuel Cells, Elsevier, 1995.
[2] W. Kock, Proceedings of the 4th International Symposium on SOFCs (SOFC-IV), The Electrochemical Society, Pennington, NJ, 1995, p. 841.
[3] E. Batawi, W. Glatz, W. Kraussler, M. Janousek, B. Doggwiler, R. Diethelm, Proceedings of the Solid Oxide Fuel Cells, The Electrochemical Society, Pennington, NJ, 1999, p. 731.
[4] S. de Souza, S.J. Visco, L.C. De Jonghe, Solid State Ionics 98 (1997) 57.
[5] S. de Souza, S.J. Visco, L.C. De Jonghe, J. Electrochem. Soc. 144 (1997) L35.
[6] H. Ishihara, H. Matsuda, Y. Takita, J. Am. Chem. Soc. 116 (1994) 3801.
[7] M. Feng, J.B. Goodenough, Eur. J. Solid State Inorg. Chem. T31 (1994) 663.
[8] P. Huang, A. Petric, J. Electrochem. Soc. 143 (5) (1996) 1644.K.
[9] T. Kadowaki, T. Shiomitsu, E. Matsuda, H. Nakagawa, H. Tsuneizumi, T. Maruyama, Solid State Ionics 67 (1993) 65.
[10] W.Z. Zhu, S.C. Deevi, Mater. Res. Bull. 38 (2003) 957.
[11] W.J. Quadakkers, J. Piron-Abellan, V. Shemet, L. Singheiser, Mater. High Temp. 20 (2) (2003) 115.
[12] T. Uehara, A. Toji, K. Inoue, M. Yamaguchi, T. Ohno, Proceedings of the Solid Oxide Fuel Cells VIII, The Electrochemical Society, Pennington, NJ, 2003, p. 914.
[13] Z. Zeng, K. Natesan, Solid State Ionics 167 (2004) 9.
[14] P. Kofstad, R. Bredesen, Solid State Ionics 52 (1992) 69.
[15] W.J. Quadakkers, H. Greiner, W. Kock, in: U. Bossel (Ed.), Proceedings of the 1st European SOFC Forum, Lucerne, 1994, p. 525.
[16] W.J. Quadakkers, H. Greiner, M. Hansel, A. Pattanaik, A.S. Khanna, W. Mallener, Solid State Ionics 91 (1996) 55.
[17] S. Linderoth, P.V. Hendriksen, M. Mogensen, J. Mater. Sci. 31 (19) (1996) 5077.

[18] M. Janousek, W. Kock, Proceedings of the Batteries for Portable Applications and Electric Vehicles, The Electrochemical Society, Pennington, NJ, 1997, p. 605.
[19] M.D. Vazquez-Navarro, J. McAleese, J.A. Kilner, Proceedings of the Solid Oxide Fuel Cells, The Electrochemical Society, Pennington, NJ, 1999, p. 749.
[20] T. Brylewski, T. Maruyama, M. Nanko, K. Przybylski, J. Therm. Anal. Calorim. 55 (1999) 681.
[21] K. Huang, P.Y. Hou, J.B. Goodenough, Solid State Ionics 129 (2000) 237.
[22] K. Huang, P.Y. Hou, J.B. Goodenough, Mater. Res. Bull. 36 (2001) 81.
[23] K. Honegger, A. Plas, R. Diethelm, W. Glatz, Proceedings of the Solid Oxide Fuel Cells VII, The Electrochemical Society, Pennington, NJ, 2001, p. 803.
[24] T. Brylewski, M. Nanko, T. Maruyama, K. Przybylski, Solid State Ionics 143 (2001) 131.
[25] W.Z. Zhu, S.C. Deevi, Mater. Sci. Eng. A 348 (2003) 227.
[26] T. Brylewski, K. Przybylski, J. Morgiel, Mater. Chem. Phys. 81 (2003) 434.
[27] T. Horita, Y. Xiong, K. Yamaji, N. Sakai, H. Yokokawa, J. Power Sources 118 (2003) 35.
[28] T. Horita, Y. Xiong, K. Yamaji, N. Sakai, H. Yokokawa, J. Electrochem. Soc. 150 (2003) 234.
[29] T. Horita, Y. Xiong, H. Kishimoto, K. Yamaji, N. Sakai, H. Yokokawa, Proceedings of the Solid Oxide Fuel Cells VIII, The Electrochemical Society, Pennington, NJ, 2003, p. 856.
[30] D. England, A. Virkar, J. Electrochem. Soc. 146 (1999) 3196.
[31] D. England, A. Virkar, J. Electrochem. Soc. 148 (2001) 330.
[32] Haynes 230 Alloy Product Brochure, Haynes International.
[33] Fuel Cell Handbook, The US Department of Energy, 2002.
[34] D. Gaskell, Introduction to Metallurgical Thermodynamics, 2nd ed., McGraw-Hill, 1981.
[35] C.Y. Li Jian, M. Yuh, Farooque, Corros. Sci. 42 (2000) 1573.
[36] G.V. Samsonov, The Oxide Handbook (Translated from Russian by C. Nigel Turton, T. Turton), IFI/Plenum Press, 1973.